Supplementary Information

Does Pre-catalyst Shape Matter in the Electrocatalytic Reduction of CO_2? Tracking Mosaicity and Porosity Development in Cu_2O Particles during Reaction

Aram Yoon[1], Fengli Yang[1], Jeffrey Poon[1], See Wee Chee[1*], Beatriz Roldan Cuenya[1*]

[1]Department of Interface Science, Fritz-Haber Institute of the Max Planck Society, Berlin 14195

*e-mail: swchee@fhi-berlin.mpg.de; roldan@fhi-berlin.mpg.de

Experimental Method

Cu_2O particle preparation

We prepared the size- and shape-controlled Cu_2O cubes and octahedrons directly on top of carbon working electrodes of liquid cell TEM chips and glassy carbon plates using electrochemical deposition. The detailed procedure is describe in ref. [1]. To obtain cubes, we applied alternating potentials between +0.2 V and +0.7 V versus the reversible hydrogen reference electrode (RHE) in 5 mM copper sulfate pentahydrate (SigmaAldrich) and 12.5 mM potassium chloride (⩾99% purity, SigmaAldrich) solution. Cu_2O octahedrons were prepared by cycling +0.25 V_{RHE} and +0.75 V_{RHE} in 5 mM copper nitrate (SigmaAldrich) + 50 mM sodium dodecyl sulfate solution (Suprapur).

In situ STEM measurement

The *in situ* TEM experiments were performed in a 300 kV Titan TEM (Thermo Fisher Scientific) operated in scanning-TEM mode using a Hummingbird Scientific Generation V Bulk Liquid Electrochemistry TEM holder with integrated Pt counter and Ag/AgCl (3M KCl) reference electrodes. The image sequences were acquired using an electron probe current of ~220 pA and at a frame rate of 1 frame per second with 1024 × 1024-pixel image resolution. The electron flux was always controlled below 3.5 e-$Å^{-2}$ s^{-1} to minimize electron beam-induced artifacts. The liquid cell TEM chips with a 50 nm thick silicon nitride membrane window and 250 nm spacer were also produced by Hummingbird Scientific. The chips have a 50-nm carbon film on the window that acts as the working electrode. The electrochemical experiments were performed using a Biologic SP-200 potentiostat. The potentials were measured against the built-in Ag/AgCl reference, calibrated against the Ag/AgCl in a beaker, and then converted to RHE using Nernst's equation. CO_2RR is performed against the same Ag/AgCl reference electrode.

The TEM holder was pre-filled with milli-Q water during cell assembly to ensure that the liquid fills the entire fluid path. After loading into the TEM, the syringe was filled with freshly saturated 0.1 M potassium bicarbonate ($KHCO_3$, ⩾99% purity, Fisher Chemicals) and introduced at a flow rate of 1.25 ml/min for 30 mins. Cyclic voltammetry from OCP to -1.1 V_{RHE} was first used to determine the onset potential for the CO_2RR, followed by chronoamperometry for up to 60 minutes at -1.0 V_{RHE}. After chronoamperometry, we stayed at open circuit potential for 10 minutes and continued imaging. Control experiments[2] as described in our previous work were performed to exclude possible beam-induced effects.

Ex situ electron microscopy measurements

Ex situ TEM characterization of the same specimen on the TEM chips was conducted before and after CO_2RR using the same microscope. For identical location imaging. The chip was rinsed in milli-Q water

after the end of the *in situ* TEM experiment and transferred back into the TEM within 10 minutes. *Ex situ* scanning electron microscopy (SEM) images of the control samples synthesized on glassy carbon plates were collected using a Thermo Scientific Apreo SEM.

Tomography measurement and reconstruction

The tomography series were collected every 1 ° from -70° to 70 ° in STEM mode. After image stack alignments, 3d reconstruction is done by using Algebraic Reconstruction Technique available in the Tomviz reconstruction software[3]. The reconstructed volume again is sliced to 60 volume slices and the projected image of each slice is converted into binary image slices by applying mean threshold (ImageJ) (Supplementary Figure 5). The porosity is calculated by a region detection function called 'regionprops' available in Matlab. A pore is defined as a dark area that exist within the enclosed polygon area that is drawn based on the assumed ideal shape. The porosity is then defined by the pore volume divided by the voxel volume (convex hull).

Electrocatalytic reduction of CO_2 and product analysis

Ex situ electrocatalysis experiments were conducted using a H-type cell, separating the cathodic and anodic compartments with a Selemion AMV ion exchange membrane (AGE Engineering Co., Ltd). A platinum mesh counter electrode (99.95%, Advent Research Materials Ltd., Oxford, UK), leak-free Ag/AgCl reference electrode, and a modified glassy carbon working electrode were used. The glassy carbon working electrode was held using a polyether ether ketone (PEEK) sample holder. As electrolyte, 0.1 M $KHCO_3$ was purified with Chelex 100 (50 gL^{-1}, Bio-Rad Laboratories) to remove trace metal impurities. Prior to the electrochemical measurements, the electrolyte was saturated with carbon dioxide (99.95%, AirLiquide Germany) by bubbling the gas for 30 min prior to the start of the experiment at an average rate of 20 mL min^{-1}, and bubbling was continued throughout the experiment. The pH of the electrolyte at carbon dioxide saturation was 6.8. The experiment was controlled by an Autolab potentiostat (PGSTAT302N). Throughout the experiments, the working electrode compartment was continuously stirred to ensure that its surface was exposed to a gas-saturated electrolyte and to prevent bubbles from blocking the reference electrode. Each electrolysis was measured for 1 hour and 15 min under chronoamperometry mode. The actual potential applied, $V_{applied}$, was corrected by: $V_{applied} = V_{initial} - iR$, with $V_{initial}$ the initial applied potential, R the sample resistance, and i the current at the $V_{initial}$, characterized by linear sweep voltammetry from -0.6 V_{RHE} to -1.1 V_{RHE} prior to chronoamperometric electrolysis.

On-line analysis of gaseous products from the cell was done with a gas chromatograph (GC, Agilent 8860), equipped with a thermal conductivity detector (TCD) and flame ionization detector (FID). Injections occurred every 15 min. Formate, acetate, and 1-propanol were detected by high performance liquid chromatography (HPLC, Shimadzu Prominence, Duisburg, Germany) with a NUCLEOGEL SUGAR 810

column with a refractive index detector (RID). Other liquid products were detected through liquid-gas chromatography (Shimadzu 2010 plus) equipped with a fused silica capillary column and a FID. All liquid products were measured after 75 minutes of electrolysis, with their FEs calculated. FEs correspond to the averaged of three separate measurements on three identically prepared but distinct samples. A description of the method used for the calculation of the FE of the gas and liquid products is described below.

Calculation of the Faradaic efficiency of gas products:

$$FE_{gas}(\%) = \frac{f_{flow} \times n \times F \times c_{gas}}{A \times j_{total} \times V_m} \times 100\%$$

FE_{gas}: Faradaic efficiency of gas product, %;

f_{flow}: flow rate of CO_2, mL min^{-1};

n: number of transferred electrons for certain product;

F: Faraday constant, 96,485 C mol^{-1}.

c_{gas}: volume ratio of gas product, determined by online GC;

j_{total}: total current density during CO2 bulk electrolysis, A cm^{-2};

A: geometric area of the electrode, cm^{-2};

V_m: the molar volume of an ideal gas at 1 atmosphere of pressure, 22,400 mL mol^{-1};

Calculation of the Faradaic efficiency of liquid products:

$$FE_{liquid}(\%) = \frac{c_{liquid} \times V \times n \times F}{Q_{total}} \times 100\%$$

FE_{liquid}: Faradaic efficiency of a liquid product, %;

c_{liquid}: the concentration of liquid products, determined by HPLC and Liquid GC, mol L^{-1};

V: the volume of the electrolyte, mL;

n: number of transferred electrons for certain product;

F: Faraday constant, 96,485 C mol^{-1}.

Q_{total}: total charge transferred during electrolysis at const. potential or current, C;

To ensure reproducibility, all the product analysis was repeated three times using identically prepared new samples. Gas chromatography (GC) provided online data every 15 minutes, and the final FE was calculated by averaging five injections across the three separate experiments. A minimum accumulation time of 15-minutes is required per GC injection due to the need to saturate

the headspace of the H-type cell. The measurement of the liquid products, which was performed after the end of the entire experiment, was repeated five times.

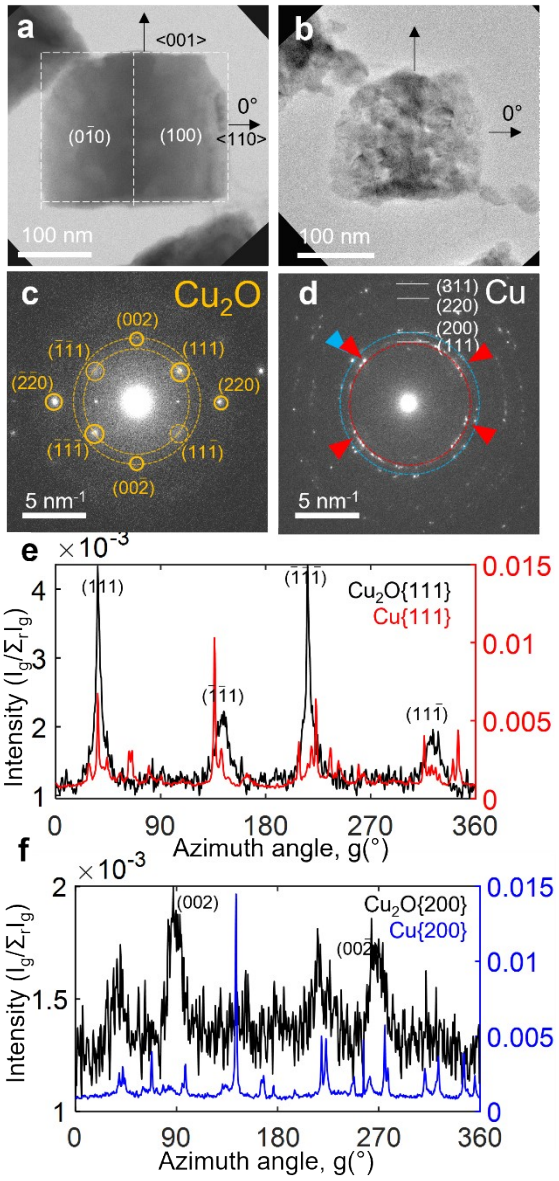

Supplementary Figure 1. Orientation relation of Cu_2O and Cu before and after CO_2RR: Cu_2O{200} ∠Cu{200} = 45° and Cu_2O {111}//Cu{111} found in another cubic particle. TEM images of cube (a) before and (b) after CO_2RR. Diffraction patterns show single crystals patterns of Cu_2O in (c), and polycrystalline ring pattern of Cu in (d). Radial intensity of Cu_2O{111} and {002} circled in yellow in (e) are plotted in black lines in (e) and (f), respectively. Radial intensity of Cu{111} (red) and Cu{200}(blue) in (d) are plotted with red line in (e) and blue line in (f).

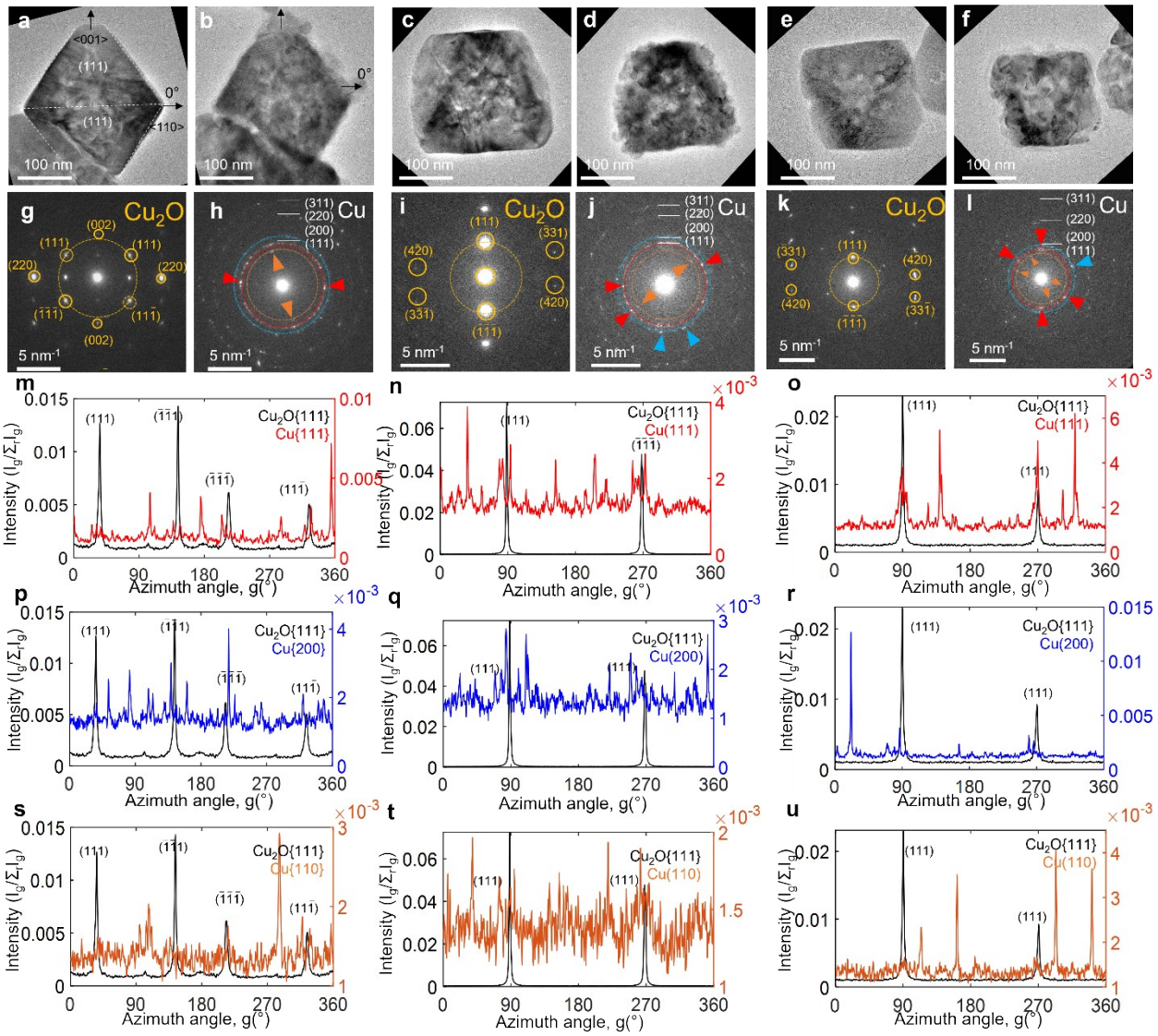

Supplementary Figure 2. Orientation relation of Cu_2O and Cu before and after CO_2RR: Cu_2O{111}//Cu{111} or Cu_2O{111}∠Cu{111} = 20~45°, found in octahedral particles. TEM images of octahedra (a), (c), and (e) before and (b), (d), and (f) after CO_2RR. Diffraction patterns show single crystals patterns of Cu_2O in (g), (i) and (k), and polycrystalline ring pattern of Cu in (h), (j) and (l). The radial intensity of Cu_2O{111} (yellow) from (e), (i) and (k) are plotted as black lines in (m) to (u). Radial intensity of Cu{110}(orange),{111} (red) and Cu{200} (blue) in (h) are plotted with red line in (m), blue line in (p), and orange line in (s). Radial intensity of Cu{110}(orange),{111} (red) and Cu{200} (blue) in (j) are plotted with red line in (n), blue line in (q), and orange line in (t). Radial intensity of Cu{110}(orange),{111} (red) and Cu {200} (blue) in (l) are plotted with red line in (o), blue line in (r), and orange line in (u).

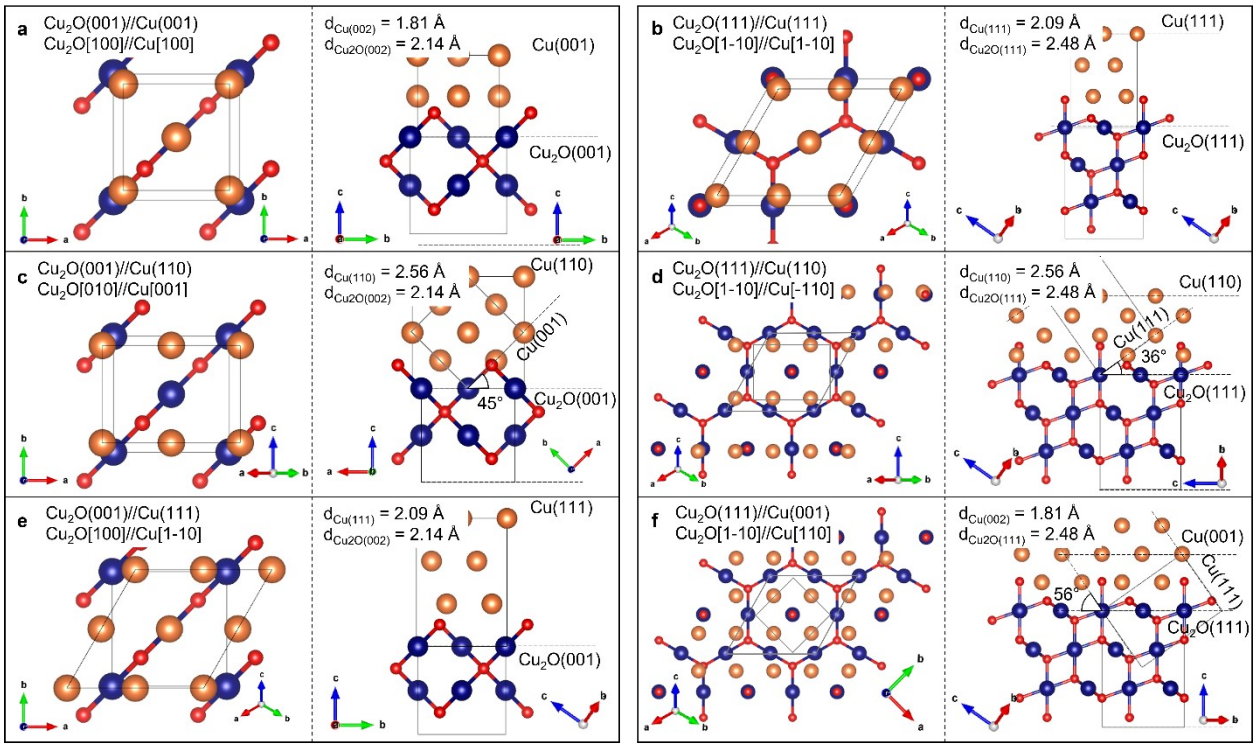

Supplementary Figure 3. Possible orientation relation of Cu_2O and Cu in top view (left) and side view (right). (Blue: Cu atoms in Cu_2O, Red: oxygen atoms in Cu_2O, and Orange: metallic Cu atoms). At orientation relation of (a) Cu_2O(001)// Cu(001), (b) Cu_2O(111)//Cu(111), (c) Cu_2O(001)//Cu(110), (d) Cu_2O (111)//Cu(110), (e) Cu_2O(001)//Cu(111), and (f) Cu_2O (111)//Cu(001). The arrows on the left bottom corner are the orientation of Cu_2O and on the right bottom corner those of Cu.

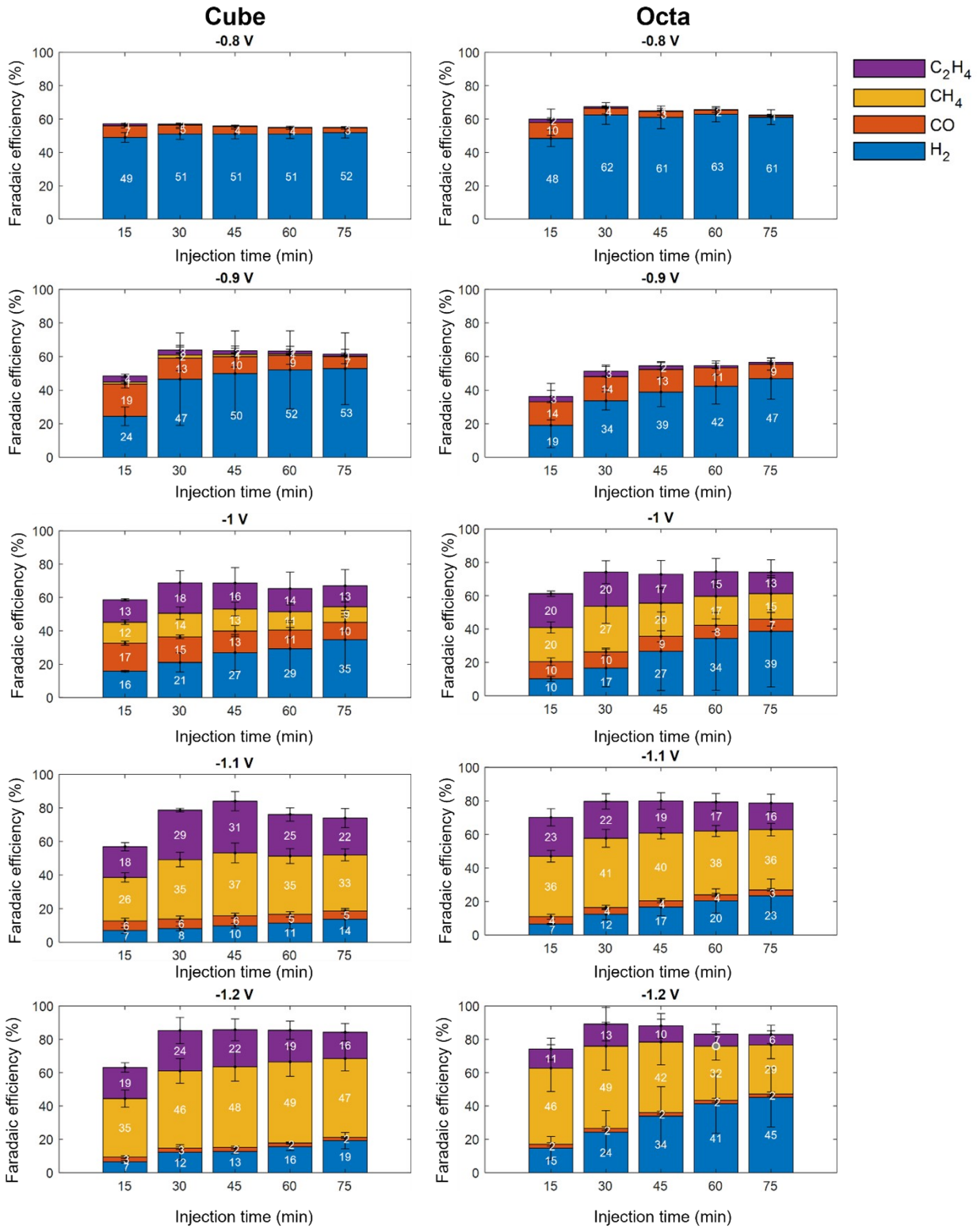

Supplementary Figure 4. Time-dependent gas product Faradaic efficiency of the shaped particles at various applied potentials (from –0.8 V to –1.2 V) in 0.1 M $KHCO_3$. Gas product measurements were taken every 15 minutes over a total duration of 75 hours. The lower FE in the first injection is explained by the headspace of the cell being insufficiently saturated.

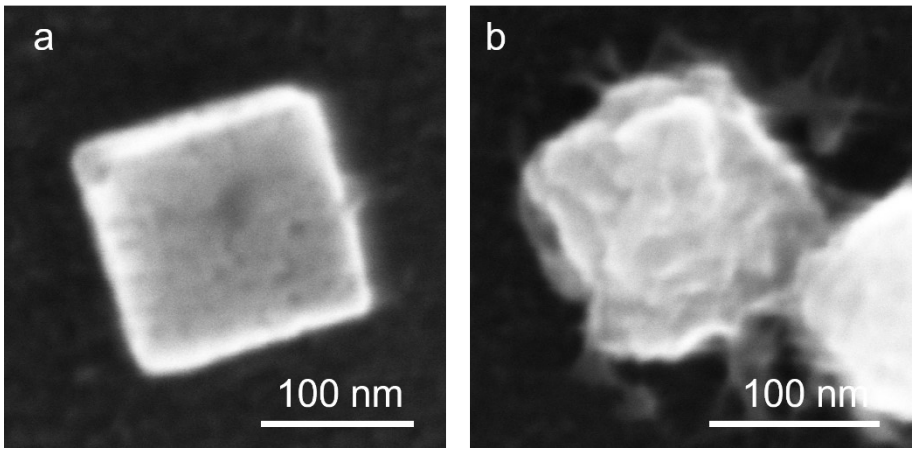

Supplementary Figure 6. SEM images of the Cu catalysts particles after CO_2RR (a) Cube and (b) Octahedron after reaction in 0.1 M $KHCO_3$ at -1.0 V_{RHE} for 1 hr.

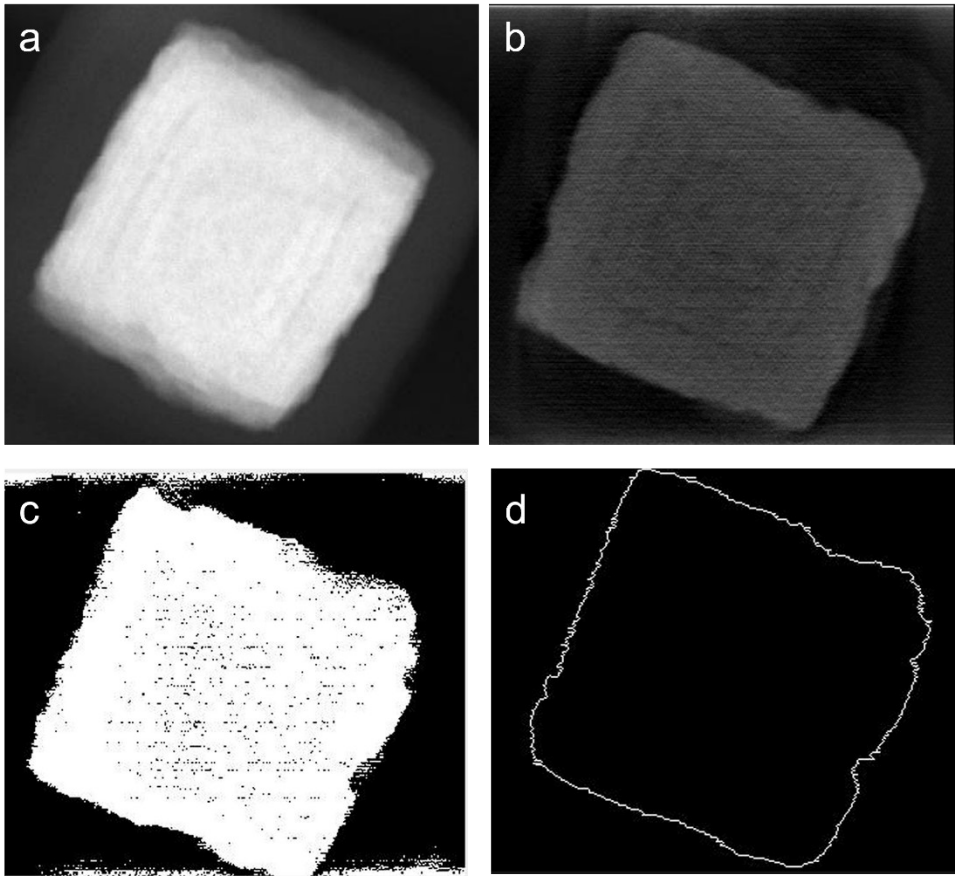

Supplementary Figure 5. Pore and surface area quantification. (a) HAADF image of the cube as deposited (raw tomography data) (b) a slice of the reconstructed 3d volume (c) binarized image of the cube to obtain the area, which is the projected area of the volume slice, (d) detected edge which represent the projected surface area of the volume slice.

References

[1] P. Grosse, A. Yoon, C. Rettenmaier, S. W. Chee, B. Roldan Cuenya, *J. Phys. Chem. C* **2020**, *124*, 26908–26915.

[2] P. Grosse, A. Yoon, C. Rettenmaier, A. Herzog, S. W. Chee, B. Roldan Cuenya, *Nat. Commun.* **2021**, *12*, 6736.

[3] "Tomviz," can be found under https://tomviz.org/.